Cyclotron resonant photoresponse of a multisubband two-dimensional electron system on liquid helium

A. O. Badrutdinov,* L. V. Abdurakhimov, and D. Konstantinov
Quantum Dynamics Unit, Okinawa Institute of Science and Technology (OIST) Graduate University, Tancha 1919-1, Okinawa 904-0495, Japan

(Received 4 March 2014; revised manuscript received 11 July 2014; published 12 August 2014)

We report an experimental study of surface electrons on liquid helium-4 under cyclotron resonant excitation. Significant resonance-induced redistribution of electron density due to overheating was observed. Analysis of redistributed charges indicates an unusually large expansion of the electron system in a lateral direction, which cannot be understood in the framework of the generally accepted effective electron temperature approximation. To interpret the data we suggest that under resonant cyclotron pumping, a fraction of nonthermalized electrons is formed, in which the average energy associated with electron in-plane motion can significantly exceed the average energy associated with motion perpendicular to the helium surface.

DOI: 10.1103/PhysRevB.90.075305 PACS number(s): 73.20.−r, 76.40.+b, 78.56.−a

I. INTRODUCTION

Surface electrons on helium (SEs) form a nondegenerate, two-dimensional electron system [1,2]. Due to confinement in a potential well, which is the sum of an attractive helium image-charge potential and a short-range repulsive potential on the surface, SE motion perpendicular to the surface is quantized, while along the surface SEs can move essentially freely. The subband energy structure of a SE system can be written as $E = -\Delta/n^2 + \hbar^2k^2/2m_e$, where $\Delta \approx 7.6$ K for helium-4, $n = 1,2,\ldots$, is the subband index, k is a two-dimensional wave vector, and m_e is the electron mass. If a magnetic field B is applied perpendicular to the surface, the spectrum of in-plane motion becomes quantized as well, forming a set of equidistant Landau levels: $E = -\Delta/n^2 + \hbar\omega_c(l + 1/2)$, where $\omega_c = |e|B/m_ec$ is the cyclotron frequency.

Resonant interaction of SEs with electromagnetic radiation that excites quantum transitions between energy levels has long been of interest from the point of view of both fundamental physics [3–6] and potential applications for quantum computing [7–9]. It has been found that SEs show a resonant conductivity response to intersubband excitation, which was attributed to electron heating, as the electron system absorbs energy from the electromagnetic field [10]. In the literature, this phenomenon is known as the "bolometric photoresponse." It has been observed in a variety of systems, including semiconductor-based, two-dimensional electron systems (2DESs) [11–15], carbon nanotube films [16], and graphene [17–20], promising potential bolometric [18] and solar energy [17] applications. Usually, hot electrons are characterized by some effective electron temperature $T_e > T$, where T is the ambient temperature. This approximation assumes that energy exchange between electrons is much faster than energy relaxation into the environment. However, deviations from T_e approximation were recently demonstrated for 2DES in high-mobility heterostructures [21], and explained by emergence of a nonequilibrium electron distribution over the discrete energy spectrum [22]. This nonequilibrium distribution has been also shown to constitute one of the mechanisms responsible for microwave-induced magnetoconductivity oscillations and zero-resistance states associated with them [23–25].

Here we demonstrate that in a SE system under cyclotron resonant (CR) excitation, bolometric photoresponse is accompanied by a significant spatial redistribution of SEs. We observe transient processes in the SE system induced by turning the excitation on and off, and reveal that under the CR condition, the distribution of SE charge differs from that in equilibrium. Two components of CR-induced redistribution are observed, corresponding to charge displacement both in the helium surface plane and perpendicular to the surface. Numerical analysis of both redistribution components in terms of the effective electron temperature T_e fails to describe the experimental data with a uniform T_e. Comparison of numerical and experimental results leads to an assumption that a fraction of nonthermalized electrons is present in the SE system under CR excitation.

II. EXPERIMENT

SEs are formed in a cylindrical, vacuum-tight cell, mounted on a dilution refrigerator, and filled with liquid helium-4. The surface of the liquid is located roughly equidistant between two parallel sets of concentric electrodes, separated by a vertical gap $d = 2.6$ mm [Fig. 1(a)]. The outer radii of electrodes in each set are 0.7, 1, and 1.3 cm, with the radial gap between them about 0.2 mm. Positive dc voltage V_B, applied to the bottom electrodes, B1 and B2, is used to control the confinement potential, thus defining the boundaries of the electron pool. Electrons are produced by briefly heating up a tungsten filament located nearby, while a certain value of $V_B = V_B^0$ is applied to the B1 and B2 electrodes, and other electrodes are grounded. The surface density of electrons n_e can be determined as $n_e = \epsilon V_B^0/2\pi|e|d$, where $\epsilon \approx 1.057$ is a dielectric constant of liquid helium-4. During the measurements, electrons were first produced at $V_B^0 = 9.65$ V, resulting in the electron density $n_e \approx 4.3 \times 10^7$ cm^{-2}. Then V_B was varied in the range 13–19 V, with corresponding variation of n_e in the range 4.5–5.0 $\times 10^7$ cm^{-2}, while the total number of SEs remained constant. In addition, an external magnetic field B was applied perpendicular to the helium

*alexbadr@oist.jp

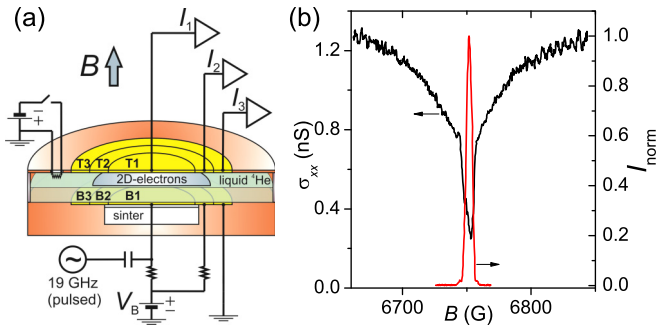

FIG. 1. (Color online) (a) Schematic view of the experimental cell and the measurement circuit used to study SE-motion-induced image-charge currents. (b) Longitudinal conductivity σ_{xx} (left axis) and normalized, demodulated image-charge current response from the T1 electrode $I_{\rm norm}$ (right axis) of the SE system under CR excitation at $T = 0.2$ K.

surface. All measurements were done at $T = 0.2$ K, where both elastic and inelastic scattering of electrons is due to their interaction with surface capillary waves (ripplons).

CR was detected by measuring SE conductivity σ_{xx} as a function of B and observing the resonant photoconductivity change [26]. Conductivity was measured by means of the capacitive coupling method, using a Corbino disk formed by electrodes T1 and T2 [Fig. 1(a)]. Electron in-plane motion was driven by applying ac voltage of 10 mV amplitude and 334 Hz frequency to the T1 electrode, and the capacitively induced response was recorded from the T2 electrode using a lock-in amplifier. In order to excite CR, continuous ac excitation of 19 GHz frequency was applied to the B1 electrode together with a constant dc voltage $V_{\rm B}$ through a dc-ac mixer.

The resonant photoconductivity response shows a complex structure consisting of a broad minimum and a narrow dip [Fig. 1(b)]. In the ripplon scattering regime, heating of SEs must decrease their conductivity as electrons populate higher subbands and move away from the liquid surface, thus decreasing their coupling to the ripplons [2]. Therefore, we attribute the observed photoconductivity response to the resonant heating of the SE system. As the strongest heating appears at the resonance, we identify the resonant field B_0 as the center of the narrow dip. The observed value of about 6750 G coincides with $B_0 = m_{\rm e}\omega_{\rm c}c/|e|$ within the error of our magnet calibration constant. The appearance of a narrow dip indicates much stronger overheating of the electron system at resonance comparing with overheating within the rest of the broad minimum of σ_{xx}. One might expect that SE states are quite different in these two regimes.

To observe the dynamic response of SEs to CR excitation, the magnetic field was set to the resonant value B_0, and an experimental circuit was assembled as shown in Fig. 1(a) (see also Ref. [27]). Pulse-modulated (100 percent modulation depth) 19 GHz excitation was applied to the B1 electrode, effectively turning the CR condition on and off. CR-induced electron dynamics has been probed by synchronous (with pulse modulation) detection of capacitively induced image-charge currents from the T1, T2, and T3 electrodes, which were amplified and then recorded using an oscilloscope. As one

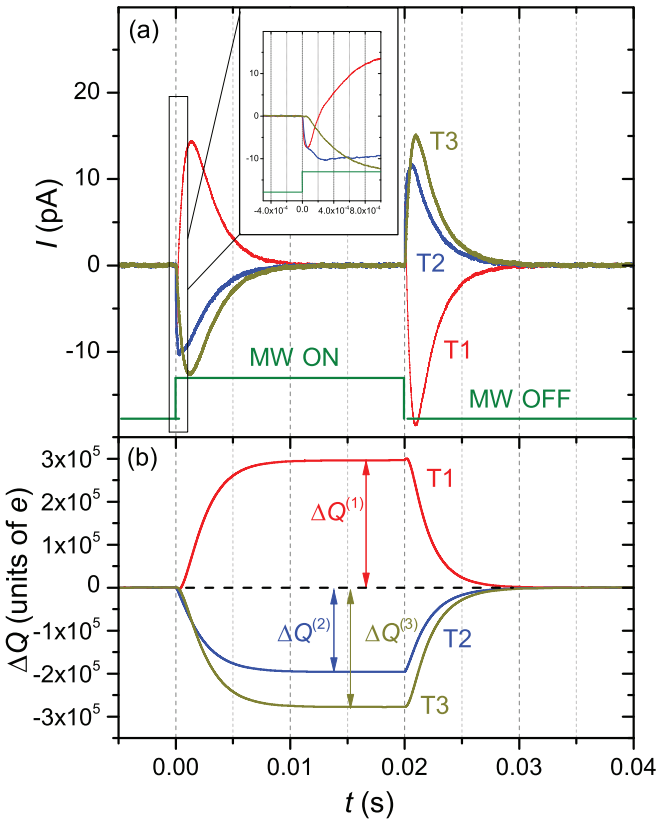

FIG. 2. (Color online) (a) Image-charge currents, induced on electrodes T1, T2, and T3, by SE motion in the sample cell due to switching CR excitation on and off, measured at $V_{\rm B} = 15$ V. Inset: Same data on a different time scale. Note: the image-charge current response may have a certain instrumental delay; thus, it may not reflect short-time dynamics precisely. (b) Corresponding changes of total image charge on electrodes $\Delta Q^{(i)}$, obtained by integration of image-charge currents over time.

can see, switching between CR-on and CR-off conditions induces nearly symmetric image-charge currents on all three T electrodes [Fig. 2(a)], indicating that electron charge distribution in the cell under CR conditions significantly differs from that at equilibrium. The range of B around its resonant value, where the redistribution appears, coincides with the width of the narrow conductivity dip. This was verified by recording demodulated, induced image-charge current as a function of B and comparing it with the photoconductivity response [Fig. 1(b)].

Careful examination of the redistribution onset [Fig. 2(a), inset] reveals the complexity of image-charge current responses. Specifically, before the dynamics visible on the main plot of Fig. 2(a) develop, image-charge currents from the T1 and T2 electrodes, upon turning CR excitation on, go negative on a much shorter time scale. At the same time, no short-term dynamics are visible in the image-charge current of the T3 electrode. Taking into account that in equilibrium all electrons are confined underneath the T1 and T2 electrodes, a qualitative picture emerges that turning on CR excitation first causes SEs to elevate from the helium surface and then a radial charge redistribution towards circumference of the SE pool occurs.

Integration of image-charge currents over time allows us to determine the total change of the image charge ΔQ on each of the electrodes [Fig. 2(b)]. It is relatively straightforward to separate contributions to ΔQ from lateral and vertical displacements of SEs. For each of the three T electrodes, we write $\Delta Q^{(i)} = \Delta Q^{(i)}_{\text{in-plane}} + \Delta Q^{(i)}_{\text{perp}}$. Then, because of SE charge conservation, we can write $\Delta Q^{(1)}_{\text{in-plane}} + \Delta Q^{(2)}_{\text{in-plane}} + \Delta Q^{(3)}_{\text{in-plane}} = 0$. Finally, $\Delta Q^{(1)}_{\text{perp}} = \Delta Q^{(2)}_{\text{perp}}$, since the surface areas of the T1 and T2 electrodes are nearly equal, and $\Delta Q^{(3)}_{\text{perp}} = 0$, since initially there are no electrons under the T3 electrode. From these six equations, we obtain six unknown values of $\Delta Q^{(i)}_{\text{perp}}$ and $\Delta Q^{(i)}_{\text{in-plane}}$.

We explored SE redistribution signals at several values of V_B in the range 13–19 V, and for each value of V_B estimated $\Delta Q^{(i)}_{\text{perp}}$ and $\Delta Q^{(i)}_{\text{in-plane}}$. Apparently, decreasing V_B leads to the increase of the amount of redistributed charge, in both in-plane and perpendicular directions [Figs. 3(a) and 3(b)].

III. NUMERICAL SIMULATION

The observed charge redistributions may originate from resonant heating of SEs: for SEs confined in a 3D potential trap and characterized by some effective electron temperature T_e, spatial distribution of charge would depend on both T_e and the confinement potential (V_B). Below we present numerical calculations, which, assuming the heating-induced redistribution scenario, allowed us to obtain the induced image charges and to compare them to the experimental data for different V_B. We define nonequilibrium 3D electron density $\tilde{n}_e(\rho,z)$ in the cylindrical coordinate system, where ρ is counted from the center of the cell, z is counted from the helium surface, and there is an azimuthal symmetry. For a given T_e, SE distribution is governed by Boltzmann statistics

$$\tilde{n}_e(\rho,z) = \tilde{n}_e(0,0)\exp\left[-\frac{e[\varphi(\rho,z)-\varphi(0,0)]}{k_B T_e}\right]. \quad (1)$$

The potential $\varphi(\rho,z)$ satisfies the Poisson equation

$$\Delta\varphi(\rho,z) = -4\pi e\tilde{n}_e(\rho,z)/\epsilon \quad (2)$$

with boundary conditions defined by V_B. Equations (1) and (2) together form a Poisson-Boltzmann equation, which must be solved to obtain $\tilde{n}_e(\rho,z)$ and $\varphi(\rho,z)$. Then the CR-induced change of the image charge at the top electrodes can be calculated as $\Delta Q^{(i)} = (1/4\pi)\int_{S^{(i)}}(E - E^{eq})ds$, where E, E^{eq} are electric fields at the top electrodes in excited and equilibrium states respectively, and $S^{(i)}$ is the surface area of the corresponding top electrode. For the equilibrium state, where $T_e = T = 0.2$ K, variations of the potential within the SE layer can be neglected. The problem reduces to solution of the Poisson equation with boundary conditions, assuming an equipotential SE layer with 2D density $n_e(\rho)$ independent on z, which is done using the Green's function method [28].

We solved the Poisson-Boltzmann equation numerically using the relaxation method. This is known to be challenging in the limit of low T_e: since small variations of $\varphi(\rho,z)$ can cause large variations of $\tilde{n}_e(\rho,z)$, the solution tends to diverge on a relatively rough grid, while introducing a fine enough grid is too computationally demanding [29]. This complication

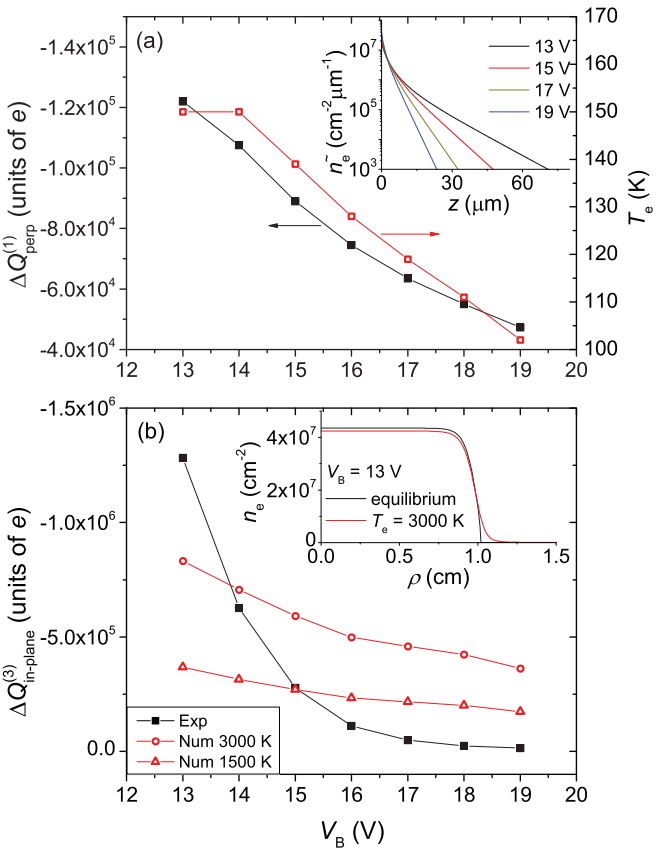

FIG. 3. (Color online) (a) Left axis: Total image charge induced on the T1 electrode by SE redistribution perpendicular to the helium surface, $\Delta Q^{(1)}_{\text{perp}}$, as a function of V_B. Right axis: T_e as a function of V_B obtained numerically by fitting each experimental point in the framework of a model described in the text. The lines are visual guides. We note that at $V_B = 13$ V, $\Delta Q^{(1)}_{\text{perp}}$ and, consequently, T_e may be underestimated, since the charge conservation condition $\sum \Delta Q^{(i)}_{\text{in-plane}} = 0$ may not hold precisely due to the change of induced charge on cell walls. Inset: Corresponding electron density $\tilde{n}_e$ as a function of z, calculated for different values of V_B. Units for $\tilde{n}_e$ are chosen to demonstrate how surface density in cm^{-2} changes on a μm scale with z. (b) Total image charge, induced on the T3 electrode by SE redistribution parallel to the helium surface, $\Delta Q^{(3)}_{\text{in-plane}}$, as a function of V_B. Solid symbols represent experimental data. Open symbols are the results of numerical calculations with T_e equal to 3000 K and 1500 K. The lines are visual guides. Inset: Radial electron density profiles calculated for cold SEs and for SEs overheated to 3000 K, at $V_B = 13$ V.

was overcome, in part, by simplifying the problem for the case of the out-of-plane redistribution. In our experimental cell geometry, in equilibrium the SE density is nearly independent of ρ everywhere other than in the vicinity of the boundary [inset of Fig. 3(b)]. This holds for the excited state as well, since the amount of charge redistributed in plane ($\sim 10^5$–10^6 electrons) is much less than the total charge of the SE system ($\approx 1.3 \times 10^8$ electrons). Thus, to model the redistribution of SEs in the z direction, perpendicular to the helium surface, a good approximation is to consider $\tilde{n}_e(\rho,z)$ and $\varphi(\rho,z)$ independent of ρ, and solve a 1D Poisson-Boltzmann equation in the z direction using the parallel plate capacitor model. This makes

the model much simpler computationally, so we solve it on a fine grid $\Delta z = 0.1$ μm and have a nice convergence even in the limit of low T_e. In the model we also presume that T_e is high enough to neglect quantization of perpendicular motion. As a result, we obtain a dependence of T_e on V_B [Fig. 3(a)]: here each data point is obtained by fitting the numerical value of $\Delta Q^{(1)}_{perp}$ induced on the T1 electrode to the corresponding experimental value. The obtained values of T_e are indeed much larger than the value of $\sim$7 K associated with quantum confinement in the z direction, justifying our assumption. The inset of Fig. 3(a) shows the estimated $\tilde{n}_e(z)$ at different values of V_B. Note that while the majority of SEs remains within a few microns of the surface, a small fraction of SEs raises appreciably.

In the case of the in-plane redistribution, we have to solve a problem in (ρ,z) space. We introduce a grid spacing $\Delta\rho = \Delta z = 50$ μm; under these conditions the solution converges only for $T_e \gtrsim 1000$ K. However it turns out that the results obtained in the limit of high T_e are sufficient to make a meaningful comparison with the experiment, as will be demonstrated shortly. We note that the estimated change of $\varphi(\rho,z)$ with z across the z profile of $\tilde{n}_e(z)$ is small (about few percent) compared to the change of $\varphi(\rho,z)$ with ρ across the boundary of the SE pool. Also, the displacement of the majority of electrons along z is much smaller than the grid spacing of this problem. Thus, it is a good approximation to disregard the out-of-plane redistribution in this problem and consider SEs to be a 2D layer, with $n_e(\rho)$ independent of z. An example of the estimated heating-induced change of $n_e(\rho)$ is shown in the inset of [Fig. 3(b)]. Experimental data for $\Delta Q^{(3)}_{in-plane}$ are compared to numerical data obtained at T_e equal to 3000 K and 1500 K, at different values of V_B [Fig. 3(b)]. Apparently, to account for the in-plane redistribution, values of T_e much higher than those relevant to the out-of-plane redistribution case are required. Also, since interpolated numerical curves cross the interpolated experimental curve at different values of V_B, strong T_e dependence on V_B is implied.

IV. DISCUSSION

To summarize, the heating-induced model with a uniform T_e fails to explain the experimental observations altogether. There is, however, a good agreement in the case of the out-of-plane redistribution. In particular, the estimate of T_e is consistent with expectations based on previous work [30]. The dependence of T_e on V_B is also expected: as the pressing field increases, interaction with ripplons becomes stronger; hence, energy relaxation becomes faster. On the other hand, the estimate of T_e in the case of in-plane redistribution is unusually high and implies strong dependence on V_B.

To explain the inconsistency, we propose the following phenomenological scenario. Thermalization within the SE system is governed by interaction with ripplons, as well as by short-range electron-electron collisions [31]. The ripplon scattering rate decreases as SEs elevate from the helium surface. The electron-electron collision rate is a function of the SE density. In case of significantly overheated SEs, having the density profile in the z direction [inset of Fig. 3(a)], both rates, and therefore the thermalization efficiency, decrease as a function of z. Thus, sparse electrons on the edge of the z profile might not be thermalized to the rest of the system. As a result, the T_e approach fails to describe their dynamics. Since the CR excitation pumps energy into the in-plane motion of electrons, the nonthermalized fraction of electrons should have an excessive energy associated with in-plane motion, while the average energy of out-of-plane motion should be about the same as that of the thermalized rest of the system. As a result, from the nonthermalized fraction we observe significant in-plane redistribution signals, while the out-of-plane redistribution signal is not affected much by its presence. The observed V_B dependence of the in-plane redistribution can be qualitatively explained by the evolution of the density profile in the z direction with V_B: as V_B decreases, more electrons can elevate well above the surface to form the nonthermalized fraction. This scenario is supported by the fact that the in-plane redistribution signal appears after the out-of-plane redistribution signal [Fig. 2(a), inset]: a certain z profile is essential for the nonthermalized fraction to appear. It is also consistent with previous discussions in the literature of so-called 3D-electron formation [30,32], based on the observation of an additional narrow line in CR absorption experiments.

It is relevant to the discussion that in our experimental setup the cyclotron excitation is not homogeneous along the SE layer. In fact, the parallel component of the ac electric field (E_{ac}) peaks around the boundary between the T1 and T2 electrodes, which might cause inhomogeneous SE heating. To evaluate the extent of the possible effect, we estimate the resonant absorption rate (Ω), and compare it to the rate of electron-electron collisions, which govern SE thermalization. The value of Ω is on the order of $|e|E_{ac}l_B/\hbar$, where $l_B = \sqrt{\hbar/m_e\omega_c}$ is the magnetic length. While it is not so straightforward to determine the actual value of E_{ac} for our experimental setup, we can infer its upper limit $\approx$37 mV/cm from the value of the microwave power at the cell input (4 μW). The obtained estimate of Ω is $\sim 10^8$ s^{-1}. Electron-electron collisions occur with a characteristic rate ω_p^2/ω_c, where $\omega_p = (2\pi e^2 n_e^{3/2}/m_e)^{1/2}$ is the plasma frequency [33]. The estimate is $\sim 5 \times 10^9$ s^{-1}. One can see that normally redistribution of energy within the SE system is much faster than energy absorption, and the system is well thermalized. However, as described in the previous paragraph, for the significantly overheated system with the density profile in the z direction, this condition may be violated for a fraction of SE, while the rest of the system still remains thermalized.

We also note that our account of other possible mechanisms that can drive electrons toward the perimeter of the pool, such as optical force [34], ponderomotive force [35], and instability due to absolute negative photoconductivity [36,37], indicates that those are not relevant for the charge redistributions we observe.

V. CONCLUSION

We observed that cyclotron resonance drives SEs on helium into a strongly overheated nonequilibrium state. Numerical simulations of the system indicate that this state cannot be described by a uniform effective electron temperature. Consistent explanation is possible within the heating-induced redistribution scenario, if we assume that there might be a

fraction of electrons not thermalized to the rest of the system. While a simple phenomenological model is proposed, more rigorous theoretical investigations of this unusual state of the SE system are highly desirable.

ACKNOWLEDGMENT

The authors are supported by an internal grant from Okinawa Institute of Science and Technology (OIST) Graduate University.

[1] E. Y. Andrei, *Electrons on Helium and Other Cryogenic Substrates* (Kluwer Academic, Dordrecht, 1997).
[2] Y. P. Monarkha and K. Kono, *Two-Dimensional Coulomb Liquids and Solids* (Springer-Verlag, Berlin, 2004).
[3] C. C. Grimes and T. R. Brown, Phys. Rev. Lett. **32**, 280 (1974).
[4] V. S. Edel'man, Zh. Eksp. Teor. Fiz. **77**, 673 (1979) [Sov. Phys. JETP **50**, 338 (1979)].
[5] D. K. Lambert and P. L. Richards, Phys. Rev. Lett. **44**, 1427 (1980).
[6] E. Collin, W. Bailey, P. Fozooni, P. G. Frayne, P. Glasson, K. Harrabi, M. J. Lea, and G. Papageorgiou, Phys. Rev. Lett. **89**, 245301 (2002).
[7] P. M. Platzman and M. I. Dykman, Science **284**, 1967 (1999).
[8] S. A. Lyon, Phys. Rev. A **74**, 052338 (2006).
[9] D. I. Schuster, A. Fragner, M. I. Dykman, S. A. Lyon, and R. J. Schoelkopf, Phys. Rev. Lett. **105**, 040503 (2010).
[10] D. Konstantinov, H. Isshiki, Y. P. Monarkha, H. Akimoto, K. Shirahama, and K. Kono, Phys. Rev. Lett. **98**, 235302 (2007).
[11] F. Neppl, J. P. Kotthaus, and J. F. Koch, Phys. Rev. B **19**, 5240 (1979).
[12] D. Stein, G. Ebert, and K. von Klitzing, Surf. Sci. **142**, 406 (1984).
[13] K. Hirakawa, K. Yamanaka, Y. Kawaguchi, M. Endo, M. Saeki, and S. Komiyama, Phys. Rev. B **63**, 085320 (2001).
[14] K. Bittkau, N. Mecking, Y. S. Gui, C. Heyn, D. Heitmann, and C.-M. Hu, Phys. Rev. B **71**, 035337 (2005).
[15] S. Komiyama, H. Sakuma, K. Ikushima, and K. Hirakawa, Phys. Rev. B **73**, 045333 (2006).
[16] M. E. Itkis, F. Borondics, A. Yu, and R. Haddon, Science **312**, 413 (2006).
[17] N. M. Gabor, J. C. W. Song, Q. Ma, N. L. Nair, T. Taychatanapat, K. Watanabe, T. Taniguchi, L. S. Levitov, and P. Jarillo-Herrero, Science **334**, 648 (2011).
[18] J. Yan, M.-H. Kim, J. A. Elle, A. B. Sushkov, G. S. Jenkins, H. M. Milchberg, M. S. Fuhrer, and H. D. Drew, Nat. Nanotechnol. **7**, 472 (2012).
[19] H. Vora, P. Kumaravadivel, B. Nielsen, and X. Du, Appl. Phys. Lett. **100**, 153507 (2012).
[20] M. Freitag, T. Low, F. Xia, and P. Avouris, Nat. Photonics **7**, 53 (2013).
[21] N. Romero-Kalmanovitz, A. A. Bykov, S. Vitkalov, and A. I. Toropov, Phys. Rev. B **78**, 085306 (2008).
[22] I. A. Dmitriev, M. G. Vavilov, I. L. Aleiner, A. D. Mirlin, and D. G. Polyakov, Phys. Rev. B **71**, 115316 (2005).
[23] M. A. Zudov, R. R. Du, J. A. Simmons, and J. L. Reno, Phys. Rev. B **64**, 201311(R) (2001).
[24] R. G. Mani, J. H. Smet, K. von Klitzing, V. Narayanamurti, W. B. Johnson, and V. Umansky, Nature (London) **420**, 646 (2002).
[25] I. A. Dmitriev, A. D. Mirlin, D. G. Polyakov, and M. A. Zudov, Rev. Mod. Phys. **84**, 1709 (2012).
[26] F. C. Penning, O. Tress, H. Bluyssen, E. Teske, M. Seck, P. Wyder, and V. B. Shikin, Phys. Rev. B **61**, 4530 (2000).
[27] D. Konstantinov, A. Chepelianskii, and K. Kono, J. Phys. Soc. Jpn. **81**, 093601 (2012).
[28] L. Wilen and R. Giannetta, J. Low. Temp. Phys. **72**, 353 (1988).
[29] F. Closa, E. Raphael, and A. D. Chepelianskii, arXiv:1212.6277v2.
[30] T. Aoki and M. Saitoh, J. Phys. Soc. Jpn. **48**, 1929 (1980).
[31] D. Ryvkine, M. J. Lea, and M. I. Dykman, Abstracts of the APS March Meeting, 2006, http://meetings.aps.org/link/BAPS.2006.MAR.V47.14
[32] V. S. Edel'man, JETP Lett. **25**, 396 (1977).
[33] M. I. Dykman, C. Fang-Yen, and M. J. Lea, Phys. Rev. B **55**, 16249 (1997).
[34] H. J. Metcalf and P. van der Straten, *Laser Cooling and Trapping* (Springer, New York, 1999).
[35] S. A. Mikhailov, Phys. Rev. B **83**, 155303 (2011).
[36] Y. P. Monarkha, Low. Temp. Phys. **37**, 655 (2011).
[37] Y. P. Monarkha, Low. Temp. Phys. **38**, 451 (2012).